

RSC Advances



This is an *Accepted Manuscript*, which has been through the Royal Society of Chemistry peer review process and has been accepted for publication.

Accepted Manuscripts are published online shortly after acceptance, before technical editing, formatting and proof reading. Using this free service, authors can make their results available to the community, in citable form, before we publish the edited article. This *Accepted Manuscript* will be replaced by the edited, formatted and paginated article as soon as this is available.

You can find more information about *Accepted Manuscripts* in the [Information for Authors](#).

Please note that technical editing may introduce minor changes to the text and/or graphics, which may alter content. The journal's standard [Terms & Conditions](#) and the [Ethical guidelines](#) still apply. In no event shall the Royal Society of Chemistry be held responsible for any errors or omissions in this *Accepted Manuscript* or any consequences arising from the use of any information it contains.

Folate appended chitosan nanoparticles augment the stability, bioavailability and efficacy of insulin in diabetic rats following oral administration

Ashish Kumar Agrawal^{1,2*}, Dileep Urimi¹, Harshad Harde¹, Varun Kushwah¹, Sanyog Jain^{1*}

¹Centre for Pharmaceutical Nanotechnology, Department of Pharmaceutics, National Institute of Pharmaceutical Education and Research (NIPER), Sector 67, S.A.S. Nagar (Mohali) Punjab-160062 INDIA

²Current affiliation: James Graham Brown Cancer Center, University of Louisville, Louisville, KY, USA

Telephone: +1-502-852-3684, Fax: +1-502-852-3842

E-mail: ashishkumar.agrawal@louisville.edu; sanyogjain@niper.ac.in

**Corresponding authors*

Abstract

The present study embarks upon the folic acid (FA) functionalization of chitosan nanoparticles and its implications on stability, oral bioavailability and hypoglycemic activity following oral administration. Folic acid functionalized chitosan nanoparticles (FA-Ch-NPs) were prepared by ionotropic gelation method by using poly(sodium 4-styrenesulfonate, PSS) as cross-linking agent. Exhaustive optimization was carried out by using 4-factor, 3-level, 2-replicates “Central Composite Design” by taking pH of chitosan solution (X1), concentration of PSS (X2), stirring speed (X3) and drug loading (X4) as independent variables while the particle size (Y1), poly dispersity index (Y2), zeta potential (Y3) and entrapment efficiency (Y4) as responses. Surface and contour profiler were generated based on maximum desirability. Morphological evaluation revealed the formation of almost spherical particles while lactose 5% w/v resulted in the formation of fluffy, easy to re-disperse cake. Developed nanoparticles exhibited sustained release up to 24h following the Higuchi model of drug release irrespective of the folic acid functionalization. Entrapped insulin was stable chemically and conformationally throughout the process and the nanoparticles exhibited excellent stability in simulated biological fluids as well as different storage conditions. Uptake studies in Caco-2 cell lines demonstrated 2.98 fold higher uptake of folic acid functionalized nanoparticles (FA-Ch-NPs) in comparison with plain Ch-NPs and remarkably higher uptake in intestinal uptake studies. Oral administration of FA-Ch-NPs demonstrated 2.13 fold higher cumulative hypoglycemia and $21.8 \pm 2.4\%$ relative bioavailability in comparison with subcutaneously administered insulin solution. Conclusively, the proposed formulation is expected to be a cost effective and easy to scalable approach for oral insulin delivery.

Key words: Insulin; Chitosan nanoparticles; Folic acid; antidiabetic efficacy.

1. Introduction

Diabetes mellitus (DM) represents a group of metabolic syndromes, characterized by chronic hyperglycemia caused by insulin secretory dysfunction, defects in insulin action or both. Over the past two decades, the prevalence and severity of DM has been increased at an epidemic rate, affecting almost all countries in the world. Currently, exogenous insulin administered through subcutaneous (SC) injection is used as the primary medication for the treatment of DM. While insulin is the major hope for the treatment of Type 1 diabetes, the current therapeutic regimen involves daily, multiple SC injections of insulin. Such repetitive, mandatory dosing not only aggravates the “injection trauma” in patients with poor compliance but causes uncontrolled hypoglycemia as well. Often, administration of insulin by SC route, is associated with severe hypoglycemic shock, in which the blood glucose reaches below the basal (normal) level.^{1, 2} All these pitfalls necessitate the development of an alternate, patient compliant therapy that will prolong the action of insulin *in vivo* while alleviating side effects associated with current therapy. Oral route is always considered as the most convenient and patient-compliant route of drug administration.³ For more than a decade, the diabetic world has been deliberately waiting for an oral insulin pill because oral route is not only more patient-compliant than the conventional parenteral routes but radically augments glucose homeostasis by mimicking physiological pattern of insulin release which involves initial passage and utilization of 50% insulin through liver (a major organ involved in glucose homeostasis), followed by peripheral action.⁴ Most importantly, oral dosage forms need not to meet specialized regulatory requirements related to issues *viz.* sterility, pyrogenicity or particulate contamination and is subsequently, cost-effective. Despite these positive attributes, oral insulin delivery is still an unmet dream for the scientific community due to the high proclivity of this protein drug towards enzymatic degradation in gastrointestinal tract (GIT) and poor intestinal permeability.⁵ Over the past years, a variety of nanocarriers have

been explored for the oral delivery of insulin. These include but not limited to liposomes⁶, polymeric nanoparticles⁷ and/or solid lipid nanoparticles.⁸ Among the different polymeric nanoparticles, chitosan have been investigated extensively due to excellent biocompatibility, biodegradability and mucoadhesive properties.^{9, 10} Chitosan nanoparticles fabricated by pristine¹¹ or modified chitosan¹² as well as in combination with other polymers¹³ have been extensively investigated for parenteral or oral delivery of insulin and other protein drugs however, poor stability in acidic environment due to excessive cationic charge is the major problem. In the present report, poor stability due to the excessive cationic charge was overcome by using poly(sodium 4-styrenesulfonate, PSS) as a cross linking agent. Additionally, folic acid was coupled with chitosan nanoparticles as a targeting ligand to have the synergistic absorption through M cells as well as folate transporters in the GIT. Thus the current report presents stable, target-specific chitosan nanoparticles for oral insulin delivery having minimum regulatory hurdles in course of their translation from bench to clinics.

2. Methods

2.1. Materials

Low molecular weight Chitosan (75-85% deacetylated), Poly(sodium 4-styrenesulfonate) (PSS, average molecular weight ~70,000), Insulin (recombinant human), Insulin-FITC (>1 mol of FITC in 1 mol of insulin), streptozotocin (STZ), acrylamide, ammonium persulphate (APS), N,N'-Methylenebisacrylamide, tetramethylethylenediamine (TEMED) were purchased from Sigma Aldrich, St. Louis, MO. Folic acid (FA) was procured from Sisco Research Lab. Pvt. Ltd., (Mumbai, India). Pancreatin and pepsin were purchased from Loba Chemie (Mumbai, India). All other reagents were of analytical grade unless otherwise mentioned. Ultrapure water (LaboStar™ ultrapure water systems, Germany) was prepared in house and used for all the experiments.

2.2. Synthesis of folate-NHS (N-Hydroxysuccinimide) ester

The active ester of FA was synthesized by following our previously reported protocol.¹ Briefly, folic acid (441 mg, 1 mmol) was dissolved in anhydrous DMSO (10 ml), following which pyridine (5 ml) was added to make the reaction mixture pH basic. DCC (N,N'-dicyclohexylcarbodiimide, 250 mg, 1.2 mmol) and NHS (140 mg, 1.2 mmol) were added to the reaction mixture and left on stirring for 24 h. The white precipitate of dicyclohexyl urea (DCU) was filtered and filtrate was poured drop-wise to an excess of ice-cold, diethyl ether (200 ml) under vigorous stirring. A reddish orange solid of activated folic acid was filtered under suction and repeatedly washed with diethyl ether to remove the traces of DMSO. Following repeated washing, air dried and used for further studies.

2.3. Preparation of chitosan nanoparticles (Ch-NPs)

Chitosan nanoparticles were prepared by ionotropic gelation method by using PSS as polyanionic crosslinking agent.¹⁴ Briefly, chitosan was dissolved in acetic acid solution (0.1 % w/v) and the pH was adjusted by drop-wise addition of NaOH (1N). PSS solution was prepared separately in distilled water and mixed with insulin solution. The PSS-insulin solution was added drop-wise to chitosan solution (1:4 v/v) under continuous stirring for 10 min. Different process variables *viz.* pH, PSS concentration, stirring speed and drug loading were taken as independent variables and optimized using central composite design by considering the particle size, polydispersity index (PDI), zeta potential (ZP) and entrapment efficiency (EE) as dependent variables.

2.4. Preparation of folic acid functionalized chitosan nanoparticles (FA-Ch-NPs)

FA-Ch-NPs were prepared by considering previously optimized parameters as constant and drop-wise addition of activated folic acid (folate-NHS ester) in different weight ratio (5-50%

w/w of chitosan) to the Ch-NPs suspension and kept on stirring for 10 min. Following stirring, the effect on particle size, PDI, ZP and EE was measured.

2.4.1. Experimental design

Process and formulation variables were optimized using 4-factor, 3-level, 2-replicates “central composite” response surface design by taking pH of chitosan solution (X1), chitosan to PSS ratio (X2), stirring speed (X3) and drug loading (X4) as explanatory variables against particle size (Y1), PDI (Y2), ZP (Y3) and EE (Y4) as response variables. Surface and contour profiler were generated and design spaces were created based on maximum desirability. The SAS JMP[®] 10.0.0 statistical software (trial version) was used for the generation and evaluation of response surface design at constant “random seed”. The response variables for 30 observations (Table S1) were performed experimentally and filled in the software. Finally, model script was run according to standard least square method and effect of screening was observed. Based on the data analysis actual by predicted plot, sorted parameter estimate, prediction profiler, surface profiler and contour profiler were generated.

2.4.2. Model validation

For model validation three different points were selected within the design space, Ch-NPs were prepared and experimental values of the responses variables were compared with the predicted values and prediction error was calculated.

2.5. Characterization of chitosan nanoformulations

The insulin loaded Ch-NPs and FA-Ch-NPs were characterized for particle size, PDI, ZP, EE and morphology. Particle size, PDI and ZP were determined by using zetasizer while the percentage of insulin entrapped was determined by measuring the concentration of free insulin in

supernatant. Briefly, 1 mL of NPs dispersion was centrifuged at 21000 rpm for 30 min, supernatant was collected and analyzed for the insulin content by using validated RP-HPLC method (Mobile Phase: Acetonitrile: water containing 0.1 % TFA (30 : 70 v/v); Isocratic elution; Flow rate: 1ml/min; Wavelength: 214; Column temperature: 40±1°C; Sample Injection Volume: 30 µl). The percentage of insulin entrapped was calculated by using the following formula^{15, 16};

$$\text{Entrapment Efficiency} = \frac{\text{Total amount of Insulin} - \text{Amount of Insulin in supernatant}}{\text{Total amount of Insulin}} \times 100$$

Shape and morphology of the developed formulations was determined using scanning electron microscopy (SEM) and transmission electron microscopy (TEM). For SEM analysis, a drop of nanoparticle dispersion of corresponding formulation was dropped on a glass coverslip formerly stick to a metallic stub by a bi-adhesive carbon tape. The drop was air-dried, coated with gold to make the surface conductive, and analyzed by SEM (S-3400N, 167 Hitachi, Japan).¹⁷ A drop of each formulation was placed over the carbon-coated grid, air dried, stained with phosphotungstic acid (1% w/v) solution, and analyzed by using TEM (Morgagni 268D, Fei Electron Optics) operated at 120 kV.^{18, 19}

2.6. Freeze drying studies

Different chitosan nanoformulations were freeze dried by our previously patented step wise freeze drying²⁰ which involves the freezing at -60°C for 8 h, primary drying at -60 to 20°C for 42 h and secondary drying at 25°C for 2 h with a constant pressure of 200 Torr at each step. A preliminary screening of different cryoprotectants viz. lactose, trehalose and mannitol was carried out at 5% w/v concentration. Lactose was finalized based on preliminary screening and further optimized for varying concentration of 2.5-10% w/v. Freeze dried formulations were examined for appearance of the cake, redispersibility index and redispersibility score.

2.7. *In vitro* release study

In vitro release study was executed in three different media Simulated Gastric Fluid (SGF, pH 1.2), Simulated Intestinal Fluid (SIF, pH 6.8) and PBS (pH 7.4) to simulate all the physiological conditions encountered following oral administration.²¹ The composition of SGF and SIF was almost same as used in section 2.5.2 except the absence of pepsin and pancreatin in SGF and SIF, respectively. Nanoparticles dispersion (20 μ L) was diluted up to 1 mL in separate micro centrifugation tubes in triplicate corresponding to each time point and kept on incubation (37°C, 80 rpm) in a shaker bath for 2 h in case of SGF, 4 h in case of SIF and 24 h in case of PBS. At predetermined time intervals, tubes were collected, centrifuged at 21,000 rpm for 30 min and supernatant was analyzed for insulin content by RP-HPLC method.

2.8. Stability studies

2.8.1. In process stability

Chemical and conformation stability of a protein molecule is the prime requirement to maintain its biological activity. During the entire process of formulation development, the insulin was subjected to varying degree of mechanical as well as chemical stress which may lead to the loss of biological activity of insulin.^{22, 23}

2.8.1.1. Chemical stability

Native polyacrylamide gel electrophoresis (Native-PAGE) was performed to assess the chemical degradation, if any. For the purpose, insulin released from different nanoformulations after incubating with phosphate buffer saline (PBS, pH 7.4 for 24 h) was separated by centrifugation at 21,000 for 30 min. The collected samples from Ch-NPs and FA-Ch-NPs were loaded in the

individual wells (stacking gel 5%, resolving gel 17%) and electrophoresed at 20 mA and 200 V. The resolved bands were visualized after staining with coomassie blue.

2.8.1.2. Conformational stability

Circular dichroism (CD) spectroscopy (J-815, JASCO, Japan) was used to access conformational integrity of insulin.²⁴ Samples were obtained similar to the section 2.8.1.1. Different samples were placed in rectangular quartz cuvette of path length 0.1 cm and scanned for CD spectrum in the far UV region of 260-190 nm. Standard insulin solution was taken as a control and average of three for each sample was taken. Baseline correction was done with blank phosphate buffer pH 7.4.

2.8.2. Stability in simulated biological fluids

The stability of chitosan nanoformulations was accessed in simulated biological fluids i.e. SGF (pH 1.2) USP XXVIII and SIF (pH 6.8) USP XXVIII.^{1, 25} Chitosan formulations (200 μ L) were diluted with SGF and SIF up to 10 mL and incubated at 37°C for 2 and 4 h in SGF and SIF, respectively. Stability of the nanoformulations was estimated by measuring the effect on size, PDI, ZP and EE.

2.9. Uptake studies

2.9.1. Caco-2 cell uptake study

Potential uptake of the developed formulations was determined in Caco-2 cell lines. Cells were grown and maintained by following our previous protocol.¹ Caco-2 cells were cultured at a density of 5×10^4 cells/well and incubated with free Insulin-FITC at 10 μ g/mL and Insulin-FITC loaded chitosan nanoparticles at 1, 3 and 10 μ g/mL for 1, 2 and 3 h. Hank's Buffered Salt (HBS) solution was used for all the dilutions and blank HBS solution was taken as a negative control.

Following incubation cells were thoroughly washed with PBS and visualized under confocal microscope [Model Olympus FV 1000]. Qualitative uptake was determined by using CLSM while quantitative uptake was determined using spectrofluorometer (FlexStation[®] 3) by measuring the fluorescence at 495 nm and 520 nm, excitation and emission wavelength of FITC-Insulin, respectively after lysing the cells by adding 200 μ L of 0.1 % Triton X-100. Furthermore, a separate group of cells was pretreated with saturated solution of folic acid to saturate the folic acid receptors present on the cell surface to elucidate the influence of this pathway on cellular uptake of folic acid functionalized chitosan nanoparticles (FA-Ch-NPs).

2.9.2. Intestinal uptake study

To further elucidate the uptake of folic acid functionalization on cellular uptake in exact physiological conditions, intestinal uptake study was designed in which free Insulin-FITC (10 μ g/mL) and Insulin-FITC loaded formulations (in equivalent concentration) were administered orally in overnight fasted Sprague-Dawley rats. After 4 h of administration, rats were sacrificed and duodenal region was dissected, washed thoroughly with Ringer's solution and circular sections of this portion were visualized by using CLSM.²⁶ Similar to the Caco-2 cell uptake studies, the influence of folic acid functionalization on cellular uptake was elucidated by administering the saturated solution of folic acid before the FA-Ch-NPs treatment to saturate the folic acid receptors.

2.9.3. Storage stability

The storage stability of lyophilized nanoformulations was determined at different temperature conditions (2-8°C, 25 \pm 2°C; 60 \pm 5% RH and 40 \pm 2°C; 75 \pm 5% RH) over a period of six months by following the different guidelines (Q1A, Q1C and Q5C) of International conference on

harmonization (ICH). After the predetermined time of one, three and six months, changes in formulation quality attributes were measured.

2.10. *In vivo* studies

Male Sprague-Dawley rats (230 ± 20 g) were procured from the central animal facility of the NIPER, India and maintained at a temperature of $25 \pm 2^\circ\text{C}$ under a 12 h light/dark cycles throughout the study. All the animal protocols were dually approved by Institutional Animal Ethics Committee (IAEC), NIPER, India. Diabetes was induced by administering STZ (55 mg/kg) intraperitoneally dissolved in ice cold citrate buffer (10 mM, pH 4.4). Following STZ treatment animals were housed for a week and animals having the blood glucose level above the 250 mg/dl were included in the study.¹

Diabetic animals were randomly distributed into five groups (n=5) and kept on overnight fasting prior to commencement of the study. Groups 1 and 2 were taken as positive and negative control and treated with subcutaneous and oral administration of insulin solution at a dose of 5 and 50 IU/kg, respectively while groups 3 and 4 were treated with Ch-NPs and FA-Ch-NPs at dose equivalent to 50 IU/Kg orally. Additionally, group 5 was pretreated with saturated solution of FA to saturate the folic acid receptors 4 h before administering FA-Ch-NPs to study the involvement of FA receptor mediated pathway in the uptake of FA-Ch-NPs. Following the treatment, blood samples (~ 300 μl) were collected through retro orbital plexus under mild anesthesia at predetermined time points (0, 1, 2, 4, 6, 8, 12, 18 and 24 h). Plasma was separated by centrifugation at 10,000 rpm for 10 min at 4°C , collected and used for the glucose and insulin estimation. Plasma glucose level was determined by glucose oxidase-peroxidase kit (AutoZyme Glucose, Accurex Biomedical Pvt. Ltd.) while plasma insulin concentration was determined

using insulin ELISA kit (ELH-Insulin-001, RayBiotech Inc. Norcross, USA) by strictly following the manufacturer protocols.

The cumulative hypoglycemia was determined by comparing the Area Under the Curve (AUC) of different treatment groups with the AUC of oral insulin using the following equation;

$$\text{Cumulative hypoglycemia (\%)} = \frac{AUC_{(\text{oral insulin})} - AUC_{(\text{treatment})}}{AUC_{(\text{oral insulin})}} \times 100$$

Pharmacological availability (PA) was determined by comparing Area Above the Curve (AAC) with dose correction as follows;

$$\text{PA (\%)} = \frac{AAC_{(\text{oral})} \times \text{Dose}_{(\text{sc})}}{AAC_{(\text{sc})} \times \text{Dose}_{(\text{oral})}} \times 100$$

Plasma insulin concentration ($\mu\text{IU/mL}$) versus time profile was generated and relative bioavailability (BA_R) was determined by using following equation;

$$\text{BA}_R (\%) = \frac{AUC_{(\text{oral})} \times \text{Dose}_{(\text{sc})}}{AUC_{(\text{sc})} \times \text{Dose}_{(\text{oral})}} \times 100$$

Where, oral and SC denotes dose administration following oral and subcutaneous routes, respectively.

2.11. *Statistical analysis*

In vitro results have been denoted as mean \pm standard deviation (SD) while *in vivo* results have been denoted as mean \pm standard error of mean (SEM). One-way analysis of variance (ANOVA) followed by Tukey-Kramer multiple comparison test was performed for statistical analysis and $p < 0.05$ was considered as statistically significant.

3. Results

3.1. Synthesis of folate-NHS ester

Activated folate-NHS ester was synthesized and characterized by using FTIR spectroscopy. Detailed characterization with peak assignment has been provided separately in supplementary material (Figure S1).

3.2. Preparation and optimization of insulin loaded Ch-NPs

3.2.1. Actual by predicted plot and sorted parameter estimate

Central composite response surface design was used for the optimization of Ch-NPs and effect of explanatory variables on response variables was studied. The experimental data was analyzed by applying statistics to establish the best fit models for the explanatory variables. The “actual by predicted plot” (Figure 1 A-D) for particle size ($R^2=0.96$), PDI ($R^2=0.98$), ZP ($R^2=0.90$), and EE ($R^2=1.00$) suggested that response variables were significantly affected by all the explanatory variables. Further, significance of explanatory variables and their allies on response variables was established by “Pareto Plot Analysis” which arranges the factors and their higher order interactions on the basis of their influence on the response variables (Figure 1 E-H). A positive value of estimate is the indication of synergistic effect while a negative value is the indication of antagonism between the factors and the responses. Speed and concentration of PSS (Figure 1 E-H) were majorly affecting all the response parameters. However, in case of zeta potential, pH was also found to play a major role.

3.2.2. Prediction profiler, response surface and contour analysis

Prediction profilers were plotted to establish maximum desirability (Figure 2). The pH of chitosan solution exhibited parabolic effect on PDI and zeta potential while had no significant

effect on particle size and PDI. Concentration of PSS and stirring speed had a parabolic effect on all the response variables and affected significantly at lower as well as higher values. Drug loading had almost insignificant effect on all the response variables. Finally, maximization of desirability by prediction profiler represented pH of chitosan solution (~5.5), PSS (0.1), speed (1800 rpm) and drug loading (20%) as optimized explanatory variables which resulted in the formulation with particle size of 267 nm, PDI of 0.181, ZP of 10 and EE of 90% at 95% of confidence level.

The response surface plots were used to study the interaction effects of two explanatory variables on responses when other factors were kept constant. Ch-NPs with desired quality attributes were obtained when pH of the chitosan solution varies in the range of 5 to 5.5, PSS concentration was close to 0.1, stirring speed was close to 1800 while drug loading was 20% (Figure 3(A-L)).

Additionally, the contour profiler was plotted and effect of two explanatory variables on all responses was evaluated (Figure 4). Colored region represents the excluded area, while white area represents the design space which is a most desirable region for developing Ch-NPs of desired quality attributes.

3.2.3. Model validation

Three different points within the design space were selected for evaluating the model and compared with the actual value for the response variables. The experimental values obtained for the experimental batches were comparable with the predicted values and within the range of 10% prediction error (Table 1).

3.3. Preparation of folate conjugated chitosan nanoparticles (FA-Ch-NPs)

Activated folic acid (Folate-NHS) was used for surface functionalization instead of using simple FA by assuming that the activated FA will remain stable over the surface during the journey of nanoparticles from oral administration to its target site. To confirm whether the FA remains stable over the surface, NPs were prepared by using FA-NHS and the pellet of NPs was repeatedly washed (5 times) with PBS 7.4 and further subjected to FTIR spectroscopy (Figure S1).

Effect of different concentration of activated FA on quality attributes of Ch-NPs is shown in Figure 5. An increase in particle size and PDI was observed upon increasing the concentration of FA. A remarkable increase in particle size and PDI was observed at higher concentration ($\geq 30\%$) however, this increase was minor at lower concentrations ($\leq 20\%$) without affecting the entrapment efficiency at all the tested concentration of FA. Therefore, FA (20% w/w) was considered as optimum for preparation of FA-Ch-NPs.

The quality attributes of final Ch-NPs and FA-Ch-NPs is shown in Table 2. Morphology determination by SEM and TEM analysis (Figure 6 A, B and C, D) further confirmed the formation of almost spherical shape particles having good correlation with the results of DLS analysis.

3.4. Freeze drying of FA-Ch-NPs

Effect of freeze drying on quality attributes of chitosan nanoformulations is shown in Table 3. On the basis of redispersibility index with different cryoprotectants, lactose was finalized as it resulted in the formation of easy to redisperse cake with good redispersibility index. Lactose (5% w/v) resulted in redispersibility index close to 1. At lower concentration (2.5%), the

redispersibility index was significantly higher ($p < 0.01$) while the difference was insignificant ($p > 0.05$) at higher concentrations ($> 5\%$ w/v) (Table 4).

3.5. *In vitro* release study

The *in vitro* release profile obtained with different insulin loaded chitosan nanoformulations is shown in Figure 7. Almost similar release profile was observed in all the media irrespective of the pH of the medium. Cumulative percentage of drug released in both the formulation approached to $\sim 75\%$ within 24 h.

FA modification did not affect the release profile significantly however it was slightly higher in PBS. Model fitting further revealed Higuchi model of drug release in both the cases irrespective of FA functionalization (Table 5).

3.6. Stability studies

3.6.1. Chemical stability

The bands position observed in native gel electrophoresis is shown in figure 8A which clearly demonstrates the absence of multiple bands and same level of bands for standard insulin and insulin extracted from Ch-NPs and FA-Ch-NPs indicative of chemical stability of insulin throughout the process.

3.6.2. Conformational stability

The overlay spectra of standard insulin and insulin extracted from different formulations is shown in Figure 8B which reveals that the spectrums obtained in case of different samples were superimposable.

3.6.3. Stability study in biological milieu

The effect of different biological media on quality attributes of chitosan nanoformulations is shown in Table 6. Bit decrease in particle size was observed following incubation in SGF while it was slightly increased upon incubation in SIF. A bit increase in PDI was observed in both the simulated fluids while the effect on zeta potential was just opposite to the effect observed in case of particle size in SGF and SIF. Almost 20-25% of entrapped insulin was lost after incubating the formulations in SGF and SIF.

3.6.4. Storage stability

Storage stability of the freeze dried FA-Ch-NPs was investigated according to ICH guidelines to have an idea about the shelf life of the developed formulations. The effect of different temperature conditions on formulation quality attributes is shown in Table 7. No significant change ($p>0.05$) in quality attributes of the FA-Ch-NPs was observed upon storage at $2-8^{\circ}\text{C}$ and $25\pm 2^{\circ}\text{C}$; $60\pm 5\%$ RH. However, significant changes ($p<0.05$) in other physicochemical properties were observed at $40\pm 2^{\circ}\text{C}$; $75\pm 5\%$ RH.

3.7. Caco-2 cell uptake studies

Remarkably higher uptake was observed in case of chitosan nanoformulations over free Insulin-FITC as evident by higher green fluorescence observed in CLSM analysis (Figure 9). Pretreatment with saturated solution of folic acid demonstrated decrease in fluorescence intensity. Time and concentration dependent cellular uptake was observed in case of different chitosan nanoformulations (Figure 10).

The cellular uptake of Insulin-FITC loaded chitosan nanoformulations was significantly higher ($P<0.001$) in comparison with free Insulin-FITC at each time point and concentration tested. FA

functionalization demonstrated 2.98 fold higher uptake in comparison with Ch-NPs at 10 $\mu\text{g/mL}$ after 3 h of incubation. Pretreatment with saturated solution of FA remarkably diminished the cellular uptake however it was still slightly higher in comparison with Ch-NPs.

3.8. Intestinal uptake study

Intestinal uptake study demonstrated remarkably higher uptake of FITC-Insulin loaded chitosan nanoformulations in comparison with free Insulin-FITC (Figure 11). A visually distinguished higher fluorescence was observed after folic acid functionalization of Ch-NPs however any specific uptake pattern/confined area of uptake could not be identified.

3.9. Pharmacodynamics (Glucose lowering potential)

Blood glucose level (% of initial value) with respect to time following the treatment with different formulations is shown in Figure 12. A sharp fall in blood glucose level was observed in positive control (SC insulin solution) which reached to its maximum within 4 h of treatment while no change in blood glucose level was observed in negative control (Oral insulin solution). A gradual decrease in blood glucose level was observed in case of Ch-NPs which reached to approximately 33% within 6 h and maintained below 80% up to 18 h. FA-Ch-NPs presented highest hypoglycemic response among all the treatment groups which reached up to 18% in 6 h and maintained below 60% up to 18 h. FA-Ch-NPs revealed almost double (2.13 folds) cumulative hypoglycemia and $21.3 \pm 1.1 \text{ BA}_R$ (Table 8) in comparison with subcutaneously administered standard insulin solution. FA-Ch-NPs, after pretreatment with saturated solution of folic acid, revealed almost similar profile to the plain Ch-NPs.

3.10. Pharmacokinetics

In the array of experimentation to prove the efficacy of proposed system pharmacokinetic studies were performed in which plasma insulin level was quantified. The FA-Ch-NPs demonstrated C_{\max} ($36.6 \pm 1.6 \mu\text{IU/mL}$) within six hour and the highest BA_R (21.8 ± 2.4) among all the treatment groups (Figure 13). Subcutaneously administered insulin exhibited highest concentration with steep increase in one hour followed by insignificant increase up to 4 h and decrease thereof. In contrast gradual increase up to 6 h and subsequent decrease was observed in case of different formulations. FA-Ch-NPs exhibited almost double AUC in comparison with subcutaneously administered insulin (Table 9).

4. Discussion

Chitosan nanoparticles have been reported for its tremendous potential in delivery of variety of bio-actives however, poor mechanical strength in biological milieu, poor storage stability and burst drug release²⁷ are the major problems which need to be addressed. As a part of preliminary screening, a variety of cross-linking agents were used and nanoparticles were tested for their stability in acidic media (SGF pH 1.2). Among the different cross-linking agents tested, PSS stabilized nanoparticles demonstrated excellent stability and hence finally selected for extensive optimization. Formulation quality attributes are quite important for system performance hence different variables were critically tested and optimized by using quality by design approach. The “actual by predicted plot” and “sorted estimate parameter” demonstrated that all explanatory variables had significant ($p < 0.0001$) effect on all the responses. Pareto plot analysis demonstrated speed as a major contributing factor in determining all the responses. Energy input in terms of stirring, during the crosslinking between chitosan and PSS is an important parameter which determine the order of interaction and subsequently size, PDI, ZP and EE of the formed

nanoparticles. Insufficient/excess amount led to the interaction mediated aggregation which resulted in higher particle size and PDI. Very high protonation at $\text{pH} \leq 5$ while lower degree of protonation at $\text{pH} \geq 6.5$, led to aggregation due to insufficient interaction with PSS molecules. Drug loading had no major impact on the formulation quality attributes however ionic interaction between oppositely charge components (negatively charged insulin molecules and positively charged chitosan) could possibly led to high entrapment efficiency (75 to 90%) at different drug loadings.

For folic acid functionalization, instead of using simple folic acid we processed with activated folic acid (folate-NHS). For the purpose, the nanoparticles pellet was washed thrice with PBS (pH 7.4) and analysed by FTIR for the presence of FA (refer supplementary material). Slight increase in particle size and bit decrease in zeta potential could be attributed to the interaction and subsequent deposition of the FA on the surface of Ch-NPs. Higher concentration (>20%) of FA resulted in significantly higher particle size and PDI and could be attributed to the concentration dependent interaction and formation of aggregates with nearby particles.

Poor storage stability is the major problem of the nanoparticles in suspension form hence to improve the storage stability nanoparticles were converted into the freeze dried form. Intact and easy to re-disperse cake observed in case of lactose could be attributed to the formation of protective network around the nanoparticles which was not strong enough in case of other cryo-protectants.

Strong electrostatic interaction between the chitosan and PSS could able to form the matrix system which was further confirmed by controlled insulin release following the Higuchi kinetic which is a typical behavior observed in case of a matrix system. Slightly higher, although

insignificant, release observed in FA-Ch-NPs in comparison with Ch-NPs at pH 7.4 might be the consequence of higher solubility of FA at basic pH.

During formulation development insulin was challenged to varying level of physical/chemical stress which might result in chemical degradation/loss of confirmation of the insulin entrapped within the system. Chemical and conformational stability of the insulin is of upmost requirement to maintain the biological activity and thus pharmacological activity of the entrapped insulin. Insulin entrapped within the nanoparticles was found chemical as well as conformationally stable indicating the suitability of designed system for the delivery of delicate drugs like insulin. Beside the stability of the entrapped insulin stability of the developed formulation in simulated biological fluids is also equally important to have the desired therapeutic performance. Strong electrostatic interaction between the positively charged chitosan molecules and negatively charged PSS could result into the formation of stable nanoparticles which was stable enough to withstand the adverse effect of harsh gastrointestinal milieu. A bit decrease in particle size in SGF and increase in particle size in SIF might be ascribed to the pH dependent solubilization of chitosan at low pH while deposition of protein over the surface in SIF. Loss of entrapped insulin up to some extent in simulated fluids could be attributed to the pH dependent solubilization and subsequent release of the entrapped insulin. Poor storage stability at higher temperature and humidity conditions ($40\pm 2^{\circ}\text{C}$; $75\pm 5\%\text{RH}$) could be attributed to temperature and humidity mediated aggregation of nanoformulations. Therefore, $2-25^{\circ}\text{C}$ and humidity up to $60\pm 5\%$ were found suitable for at least 6 months storage without compromising with the quality of the product however, real time storage is recommended to determine the exact shelf life.

The selection of Caco-2 cells to elucidate *in vitro* cellular uptake was based on the unique property of these cells to spontaneously differentiate into monolayers of polarized cells that

resemble intestinal enterocytes.²⁸ Almost non-detectable fluorescence observed in case of Insulin-FITC could be attributed to the pitiable penetrability and subsequent poor uptake due to high molecular weight. Insulin-FITC loaded Ch-NPs could enhance the cellular uptake which might be ascribed to the penetration enhancement property of chitosan. Further, folic acid functionalization could enhance the uptake by 2.98 folds which clearly demonstrate the presence of alternative uptake path for FA-Ch-NPs. Uptake of FA-Ch-NPs through additional alternative path was further confirmed by pretreatment with saturated solution of folic acid as pretreatment resulted in the comparable cellular uptake (although slightly higher) to Ch-NPs after pretreatment. Although we speculated the 100% saturation of the folic acid receptors yet, complete saturation is not possible practically and this might be the reason of slightly higher cellular uptake observed in comparison to the plain Ch-NPs even after pretreatment with folic acid. To further establish the efficacy *in vivo*, intestinal uptake study was performed which further demonstrated uniform higher fluorescence throughout the intestinal region (Figure 11) and might be the consequence of cellular uptake through transcellular as well as paracellular route. In line with the results of Caco-2 cell, pretreatment with saturated solution of FA could able to saturate the FA receptors available across the intestine and hence reduced fluorescence (Figure 11D).

To further elucidate the effect of FA modification, glucose lowering potential and pharmacological availability following oral administration was determined. Orally administered insulin solution could not lower the glucose level and might be ascribed to the obvious reason of enzymatic degradation and poor permeability across the gastrointestinal region. A sharp fall in blood glucose level, observed in case of subcutaneous administration, might be the consequence of availability of the insulin in a single shot. The better hypoglycemic response observed in case

of PSS stabilized Ch-NPs could be attributed to the better protection of entrapped insulin against gastric degradation. This observation can also be correlated with our *in vitro* stability results in which PSS stabilized Ch-NPs were found quite stable in simulated gastric conditions. There are certain reports in which nanoparticles have been reported to follow additional uptake through specialized region i.e. M-cells in Peyer's patches.²⁹ Thus better hypoglycemic response observed in case of Ch-NPs as compared to control could be attributed to the combined effect of better protection and enhanced uptake through specialized mechanisms. In line with the results of Caco-2 cell and intestinal uptake studies, folic acid modification could result into significantly higher ($P < 0.01$) hypoglycemia as compared to plain Ch-NPs indicating the presence of additional uptake mechanism involved in case of FA-Ch-NPs. This was further confirmed by the concept of pre-saturation which demonstrated similar glucose lowering profile to the plain Ch-NPs. A bit improved glucose lowering potential observed even after pretreatment could be ascribed to the practical inability to saturate all the receptors following pretreatment. To further evaluate the efficacy pharmacokinetic studies were performed in which plasma insulin level was determined. Non detectable amount observed in case of oral insulin could be ascribed to the obvious reason of enzymatic degradation and poor penetration. Folic acid modification (FA-Ch-NPs) revealed relative bioavailability of $21.8 \pm 2.4\%$ which supports the exceptional appropriateness of the proposed strategy for oral insulin delivery. Also the proposed system exhibited remarkably improved performance over already reported systems.^{5, 11, 30} An excellent PK/PD correlation is also evidenced by PA of antidiabetic activity and BA_R of pharmacokinetics. Results were also comparable to our previous observation with FA-PEG-PLGA nanoparticles and FA-layersomes.^{1, 31}

5. Conclusion

In the current report stable chitosan nanoparticles were developed in a single step by ionotropic gelation method and further evaluated for their targeting potential by appending folic acid as targeting ligand. Extensive optimization by using quality by design approach resulted in the formation of FA-Ch-NPs with particle size ~ 285 nm, PDI ~ 0.24 , zeta potential ~ 9 and entrapment efficiency $\sim 90\%$. FA-Ch-NPs demonstrated excellent stability in simulated biological fluids by maintaining the chemical and conformational stability of the insulin entrapped with the nanoparticles. In line with the hypothesis folic acid functionalization could result into 2.98 folds appreciation in cellular uptake as compared to Ch-NPs. Moreover, FA-Ch-NPs demonstrated 2.13 fold higher cumulative hypoglycemia and $21.8 \pm 2.4\%$ relative bioavailability as compared to subcutaneously administered insulin solution. Although data in hands is preliminary yet cost effectiveness, ease of scale up and negligible regulatory hurdles can make the proposed formulation strategy a clinical reality.

Acknowledgement

Authors AKA and VK are thankful to Council of Scientific & Industrial Research (CSIR), New Delhi, India for financial assistance and Director, NIPER, for providing infrastructure facilities. Authors are also thankful to Mr. Rahul Mahajan and Mr. Vinod Kumar for technical assistance in SEM and TEM analysis, respectively.

References

1. A. K. Agrawal, H. Harde, K. Thanki and S. Jain, *Biomacromolecules*, 2014, **15**, 350-360.
2. V. K. Rai, N. Mishra, A. K. Agrawal, S. Jain and N. P. Yadav, *Drug deliv*, 2014, doi:10.3109/10717544.10712014.10991001.
3. A. K. Jain, N. K. Swarnakar, C. Godugu, R. P. Singh and S. Jain, *Biomaterials*, 2011, **32**, 503-515.
4. V. Agarwal and M. A. Khan, *Pharm Technol*, 2001, 76-90.
5. K. Sonaje, Y. H. Lin, J. H. Juang, S. P. Wey, C. T. Chen and H. W. Sung, *Biomaterials*, 2009, **30**, 2329-2339.
6. Z. H. Wu, Q. N. Ping, Y. Wei and J. M. Lai, *Acta Pharmacol. Sin.*, 2004, **25**, 966-972.
7. S. Sajeesh and C. P. Sharma, *Int J Pharm*, 2006, **325**, 147-154.
8. B. Sarmiento, S. Martins, D. Ferreira and E. B. Souto, *Int J Nanomedicine*, 2007, **2**, 743-749.
9. A. Agrawal, P. Gupta, A. Khanna, R. Sharma, H. Chandrabanshi, N. Gupta, U. Patil and S. Yadav, *Pharmazie*, 2010, **65**, 188-193.
10. A. K. Agrawal, M. Das and S. Jain, *Exp Opin Drug Deliv*, 2012, **9**, 383-402.
11. Y. Pan, Y. J. Li, H. Y. Zhao, J. M. Zheng, H. Xu, G. Wei, J. S. Hao and F. D. Cui, *Int J Pharm*, 2002, **249**, 139-147.
12. L. Yin, J. Ding, C. He, L. Cui, C. Tang and C. Yin, *Biomaterials*, 2009, **30**, 5691-5700.
13. Y. H. Lin, F. L. Mi, C. T. Chen, W. C. Chang, S. F. Peng, H. F. Liang and H. W. Sung, *Biomacromolecules*, 2007, **8**, 146-152.
14. Z. Ma, H. H. Yeoh and L. Y. Lim, *J Pharm Sci*, 2002, **91**, 1396-1404.
15. H. Harde, A. K. Agrawal and S. Jain, *Pharm Res*, 2015, **32**, 122-134.
16. H. Harde, A. K. Agrawal and S. Jain, *Nanomedicine*, 2014, **9**, 2511-2529.

17. S. Jain, S. R. Patil, N. K. Swarnakar and A. K. Agrawal, *Mol Pharmaceutics*, 2012, **9**, 2626-2635.
18. S. Jain, H. Harde, A. Indulkar and A. K. Agrawal, *Nanomedicine: NBM.*, 2014, **10**, 431-440.
19. S. Jain, S. Kumar, A. Agrawal, K. Thanki and U. Banerjee, *RSC Adv*, 2015, **5**, 41144-41154.
20. S. Jain, D. Chauhan, A. Jain, N. Swarnakar, H. Harde, R. Mahajan, D. Kumar, P. Valvi, M. Das and S. Datir, *2011 filed on September*, 2011, **6**.
21. H. Harde, A. K. Agrawal and S. Jain, *J Biomed Nanotechnol.*, 2015, **11**, 363-381.
22. M. van de Weert, W. E. Hennink and W. Jiskoot, *Pharm Res*, 2000, **17**, 1159-1167.
23. H. Harde, K. Siddhapura, A. K. Agrawal and S. Jain, *Nanomedicine*, 2015, **10**, 1077-1091.
24. H. Harde, A. K. Agrawal and S. Jain, *Drug Deliv Transl Res*, 2015, **5**, 498-510.
25. S. Jain, A. Indulkar, H. Harde and A. K. Agrawal, *J Biomed Nanotechnol*, 2014, **10**, 932-947.
26. S. McClean, E. Prosser, E. Meehan, D. O'Malley, N. Clarke, Z. Ramtoola and D. Brayden, *Eur J Pharm Sci*, 1998, **6**, 153-163.
27. T. Lopez-Leon, E. L. Carvalho, B. Seijo, J. L. Ortega-Vinuesa and D. Bastos-Gonzalez, *J Colloid Interf Sci*, 2005, **283**, 344-351.
28. Z. S. Ma and L. Y. Lim, *Pharm Res*, 2003, **20**, 1812-1819.
29. H. Harde, M. Das and S. Jain, *Expert Opin Drug Deliv*, 2011, **8**, 1407-1424.
30. F. Cui, K. Shi, L. Zhang, A. Tao and Y. Kawashima, *J Control Release*, 2006, **114**, 242-250.

31. S. Jain, V. V. Rathi, A. K. Jain, M. Das and C. Godugu, *Nanomedicine*, 2012, **7**, 1311-1337.

List of Tables**Table 1: Validation of central composite model**

pH	PSS (%)	Speed	Loading	Actual by predicted	Particle size (nm)	PDI	ZP	%EE
5.5	0.1	1800	20	Predicted	267	0.181	10.0	90.4
				Actual	255 ± 7	0.193 ± 0.008	10.9 ± 0.3	89.7 ± 1.1
				Prediction error	4.32	6.99	8.79	0.69
5	0.1	1800	15	Predicted	287	0.211	10.6	92.8
				Actual	278 ± 6	0.217 ± 0.006	11.4 ± 0.9	90.4 ± 1.3
				Prediction error	3.16	3.15	6.94	2.51
5.7	0.1	1800	20	Predicted	288	0.2	9.9	89.9
				Actual	282 ± 7	0.213 ± 0.004	10.6 ± 0.7	88.1 ± 1.7
				Prediction error	2.29	6.83	6.85	1.92

Table 2: Quality attributes of chitosan formulations

Formulation	Particle size (nm)	PDI	Zeta potential (mV)	EE (%)
Ch-NPs	255.6 ± 7.7	0.193 ± 0.008	10.9 ± 0.3	89.7 ± 1.1
FA-Ch-NPs	284.9 ± 3.2	0.236 ± 0.005	8.9 ± 0.3	89.5 ± 0.9

Table 3: Preliminary screening of different cryoprotectants based on redispersibility index and reconstitution score for lyophilization of Ch-NPs and FA-Ch-NPs

Cryo-protectant	Ch-NPs			FA-Ch-NPs		
	PS (nm)	Ri=(Sf/Si)	RS	PS (nm)	Ri=(Sf/Si)	RS
Nil	255.6 ± 7.7	-	-	284.9 ± 3.2	-	-
Lactose	270.6 ± 3.2	1.05 ± 0.01	***	294.5 ± 3.7	1.03 ± 0.01	***
Trehalose	385.5 ± 7.2	1.50 ± 0.02	***	463.9 ± 9.6	1.62 ± 0.03	***
Mannitol	ND	-	ND	ND	-	ND

PS-Particle size, Ri-Redispersibility index, RS-Reconstitution score, ND-Not determined (***) redispersible within 20 sec with mere mixing). Values are presented as mean ± SD (n=6).

Table 4: Optimization of lactose concentration based on redispersibility index and reconstitution score for lyophilization of Ch-NPs and FA-Ch-NPs

Conc.	Ch-NPs			FA-Ch-NPs		
	PS (nm)	Ri=(Sf/Si)	RS	PS (nm)	Ri=(Sf/Si)	RS
Nil	255.6 ± 7.7	-	-	284.9 ± 3.2	-	-
2.5	306.1 ± 10.8	1.19 ± 0.04	***	318.2 ± 14.5	1.11 ± 0.05	***
5	270.6 ± 3.2	1.05 ± 0.01	***	294.5 ± 3.7	1.03 ± 0.01	***
7.5	275.5 ± 5.2	1.07 ± 0.02	***	296.5 ± 6.2	1.04 ± 0.03	***
10	270.1 ± 4.8	1.05 ± 0.01	***	295.0 ± 7.6	1.03 ± 0.02	***

PS-Particle size, Ri-Redispersibility index, RS-Reconstitution score, (***) redispersible within 20 sec with mere mixing). Values are presented as mean ± SD (n=6).

Table 5: Kinetic models used for analysis of insulin release from different formulations and overall correlation coefficient (R^2)

Release model	Correlation coefficient (R^2)	
	Ch-NPs	FA-Ch-NPs
Zero order	0.887	0.887
First order	0.9653	0.968
Hixson–Crowell	0.9733	0.974
Weibull	0.9733	0.974
Higuchi	0.9909	0.991
Baker–Lonsdale	0.9823	0.982
Korsmeyer–Peppas	0.9733	0.974

Table 6: Effect of simulated biological fluids on formulation quality attributes

Parameters	Size (nm)	PDI	Zeta potential (mV)	Drug entrapped (%)
Ch-NPs				
Initial	255.6±7.7	0.193±0.008	10.9±0.3	89.7±1.1
SGF pH 1.2	240.8±2.6	0.212±0.013	13.5±1.1	69.8±1.5
SIF pH 6.8	269.5±4.5	0.233±0.007	6.3±1.1	68.7±1.2
FA-Ch-NPs				
Initial	284.9±3.2	0.236±0.005	8.9±0.3	89.5±0.9
SGF pH 1.2	261.7±7.0	0.250±0.001	10.6±0.5	65.2±2.0
SIF pH 6.8	292.0±3.8	0.252±0.003	5.2±0.5	64.1±1.4

Values are presented as (mean ± SD) (n=5)

Table 7: Storage stability of FA-Ch-NPs following the storage at different temperature and humidity conditions up to six months

Months	Storage conditions		Particle size (nm)	PDI	ZP (mV)	%EE
	Temp./Humidity					
0	Initial		294.5 ± 3.7	0.242 ± 0.012	8.9 ± 0.3	89.3 ± 0.9
	2-8°C		295.2 ± 2.9	0.241 ± 0.018	8.4 ± 0.6	89.1 ± 1.2
1	25±2°C; 60±5%RH		297.3 ± 3.2	0.243 ± 0.013	8.2 ± 0.9	88.6 ± 2.3
	40±2°C; 75±5%RH		347.8 ± 9.2	0.267 ± 0.024	7.6 ± 0.7	86.5 ± 1.8
3	2-8°C		296.6 ± 3.9	0.042 ± 0.024	8.7 ± 0.9	88.4 ± 1.6
	25±2°C; 60±5%RH		301.2 ± 2.8	0.244 ± 0.019	7.9 ± 0.8	88.2 ± 2.2
	40±2°C; 75±5%RH		392.4 ± 9.7	0.301 ± 0.026	6.2 ± 0.6	84.6 ± 1.8
6	2-8°C		298.2 ± 4.1	0.240 ± 0.024	8.5 ± 0.4	88.9 ± 1.4
	25±2°C; 60±5%RH		304.6 ± 6.4	0.246 ± 0.026	7.4 ± 0.3	87.8 ± 2.1
	40±2°C; 75±5%RH		442.8 ± 12.6	0.328 ± 0.023	5.1 ± 0.6	80.4 ± 1.6

Table 8: Pharmacodynamic parameters following subcutaneous administration of insulin solution (5 IU/kg) and oral administration of insulin solution, and insulin loaded Ch-NPs, FA-Ch-NPs (50 IU/kg) with and without treatment of folic acid

Treatment groups	Dose (IU/kg)	AUC	Cumulative Hypoglycemia (%)	PA (%)	T _{max} (h)	C _{min} (% of initial value)
Insulin solution oral	50	2494.3±53.6	-	-	-	92.1±3.0
Insulin solution (SC)	5	1863.7±12.3	25.2±1.7	100	4	14.3±1.6
Ch-NPs	50	1520.6±18.3	39.0±1.5	15.4±0.8	6	32.7±2.0
FA-Ch-NPs	50	1150.2±16.6	53.8±1.2	21.3±1.1	6	17.4±1.7
FA-Ch-NPs Pretreated	50	1449.8±24.4	41.8±1.4	16.5±0.3	6	28.7±2.5

T_{max} : time at which minimum relative glucose level was observed; C_{min} minimum basal glucose value. Data is represented as mean ± SEM (n=5)

Table 9: Pharmacokinetic parameters of different treatment groups

Treatment group	Dose (IU/kg)	AUC (μIU.h/mL)	BA_R (%)	T_{max} (h)	C_{max} (μIU/mL)
Insulin SC	5	203.9 \pm 9.0	100	4	42.6 \pm 1.4
Ch-NPs	50	258.7 \pm 8.7	15.8 \pm 2.7	6	28.6 \pm 1.7
FA-Ch-NPs	50	356.5 \pm 9.5	21.8 \pm 2.4	6	36.6 \pm 1.6
FA-Ch-NPs (Pretreated)	50	276.1 \pm 10.3	16.9 \pm 2.8	6	29.2 \pm 1.8

AUC-Area under the curve; BA_R-Relative bioavailability. Results are represented as mean \pm SEM (n=5).

List of Figures

Figure 1: Actual by predicted plot for (A) particle size, (B) PDI (C) ZP and (D) %EE and pareto plot analysis arranging the factors on the basis of their influence on (E) particle size (F) PDI (G) ZP and (H) %EE.

Figure 2: Prediction profiler and maximum desirability at 95% of confidence level showing the effect of explanatory variables on responses.

Figure 3: Response surface profile representing the effect of two explanatory variables on each response where A to C represents effect on size, D to F represents effect on PDI, G to I represents effect on ZP and J to L represents effect on %EE of the combination of pH and PSS, pH and speed, pH and loading.

Figure 4: Contour profiler representing desirable “design space (white region)” based on effect of explanatory variables on responses.

Figure 5: Effect of folic acid functionalization on (A) particle size and PDI (B) zeta potential and %EE.

Figure 6: Morphology studies by using SEM (A) and (B) and TEM (C) and (D) of Ch-NPs and FA-Ch-NPs.

Figure 7: Comparative release profile of Ch-NPs and FA-Ch-NPs in different bio-mimetic media (A) SGF (pH 1.2) (B) SIF (pH 6.8) and (C) PBS (pH 7.4).

Figure 8: Chemical and conformational stability (A) Resolved bands obtained in gel electrophoresis for (I) standard insulin solution and insulin extracted from (II) Ch-NPs and (III) FA-Ch-NPs (B) Overlay CD spectra of different insulin samples.

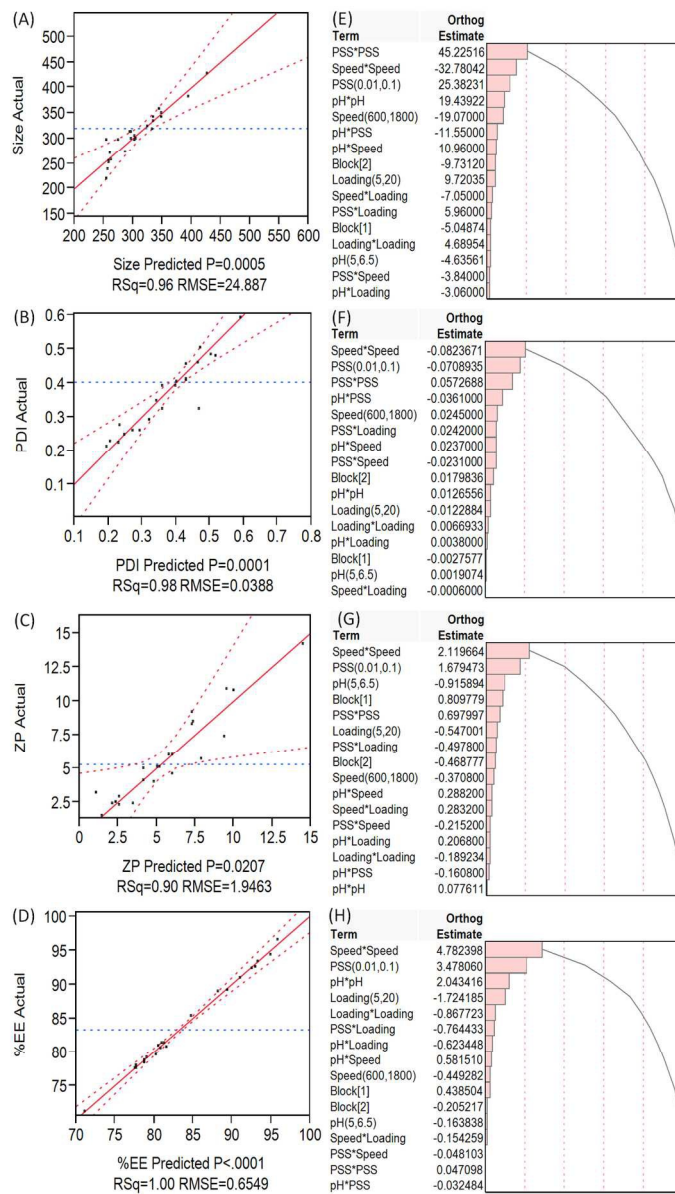
Figure 9: Representative confocal micrographs of Caco-2 cell monolayers co-incubated for 3 h with (A) free Insulin-FITC and Insulin-FITC loaded (B) Ch-NPs (C) FA-Ch-NPs (D) FA-Ch-NPs pretreated with excess of folic acid.

Figure 10: Plot indicates % uptake with respect to time in Caco-2 cell monolayers co-incubated with free Insulin-FITC and Insulin-FITC loaded Ch-NPs, FA-Ch-NPs, and FA-Ch-NPs pretreated with excess of FA for 1, 2 and 3 h at 1, 3 and 10 µg/mL. (a indicate comparison of FA-Ch-NPs with Ch-NPs after 3 h, *P<.001)**

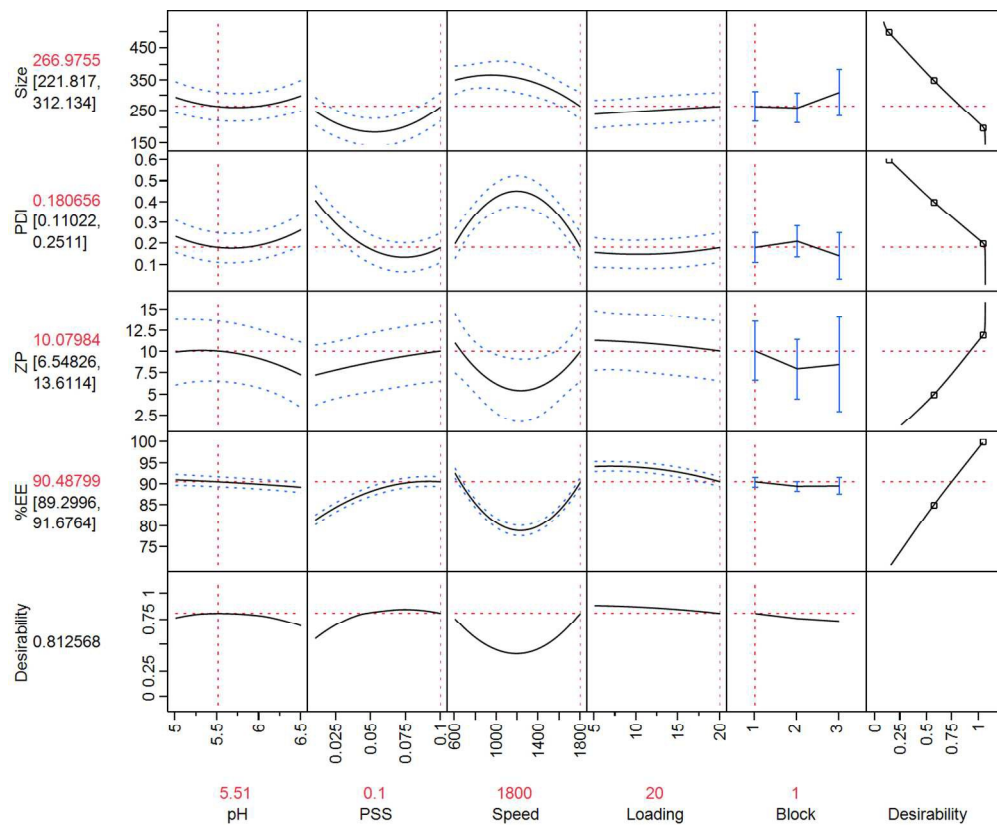
Figure 11: Representative confocal micrographs of intestinal cross sections following oral administration of (A) Free Insulin-FITC and Insulin-FITC loaded (B) Ch-NPs (C) FA-Ch-NPs and (D) FA-Ch-NPs pretreated with excess of folic acid. First half of each figure represents florescent images while other half represents overlay images. White, yellow and red arrows indicate the mucosal, submucosal and muscular regions, respectively.

Figure 12: Plot indicates the blood glucose level remaining with respect to time following subcutaneous administration of standard insulin solution (5 IU/kg) and oral administration of insulin solution, Ch-NPs and FA-Ch-NPs (50 IU/kg) with and without pretreatment with saturated solution of folic acid. (a, b and c indicate the FA-Ch-NPs as compared to oral insulin solution, Ch-NPs and SC insulin, *P<0.001, **P<0.01, *P<0.05) Data is represented as mean± SEM (n= 5).**

Figure 13: Pharmacokinetic profile following subcutaneous administration of standard insulin solution and oral administration of insulin loaded Ch-NPs, FA-Ch-NPs with and without pretreatment with folic acid. (a and b the FA-Ch-NPs as compared to Ch-NPs and SC insulin, **P<0.01, *P<0.05). Data is represented as mean± SEM (n= 5).



106x185mm (300 x 300 DPI)



122x99mm (300 x 300 DPI)

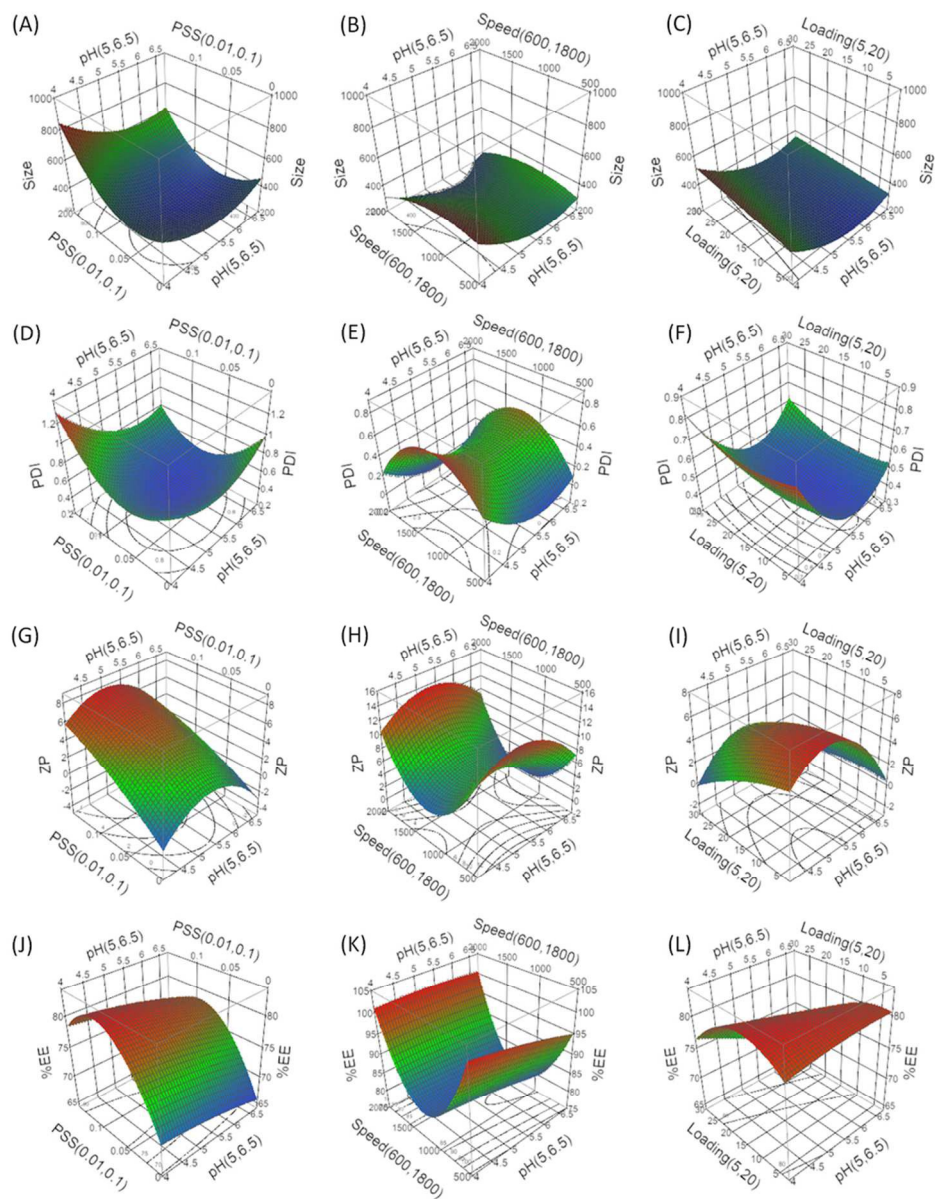
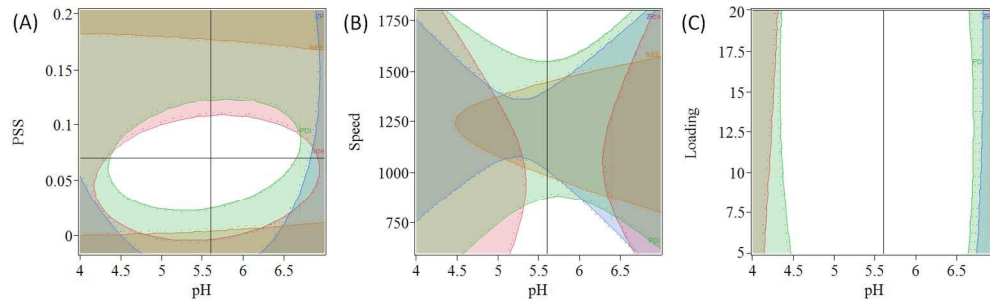
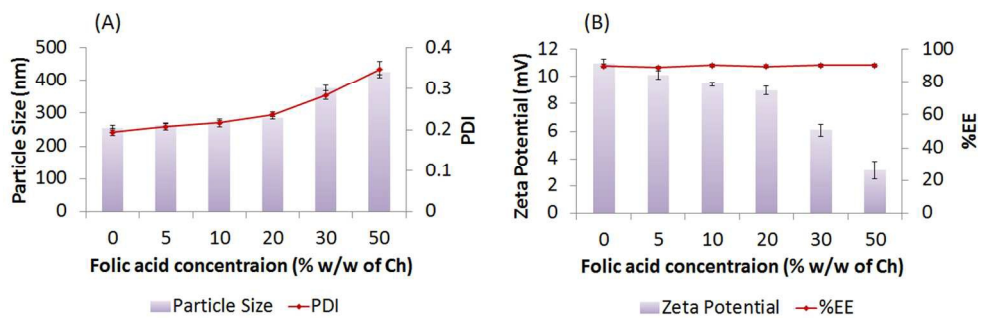


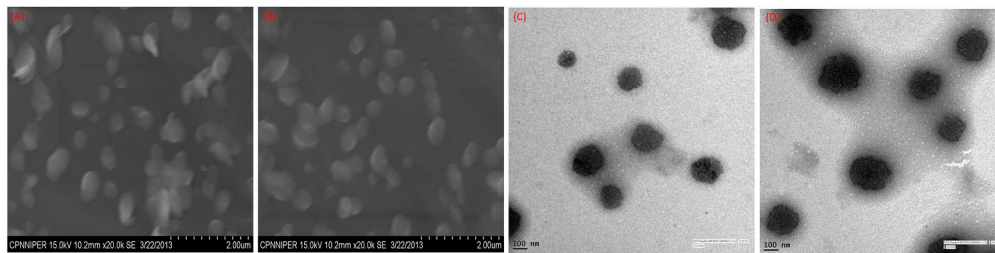
Figure 3: Response surface profile representing the effect of two explanatory variables on each response where A to C represents effect on size, D to F represents effect on PDI, G to I represents effect on ZP and J to L represents effect on %EE of the combination of pH and PSS, pH and speed, pH and loading. 85x107mm (300 x 300 DPI)



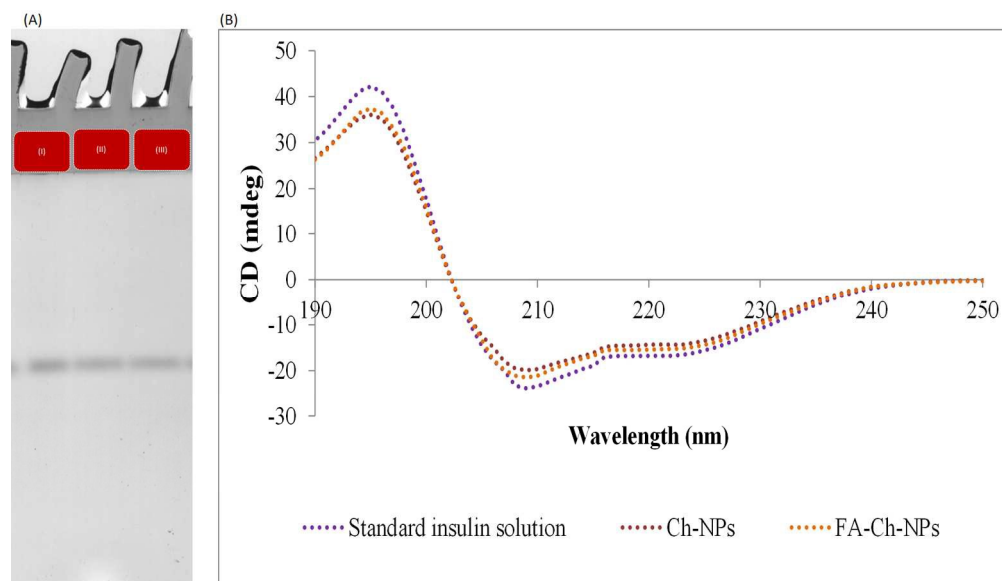
151x45mm (300 x 300 DPI)



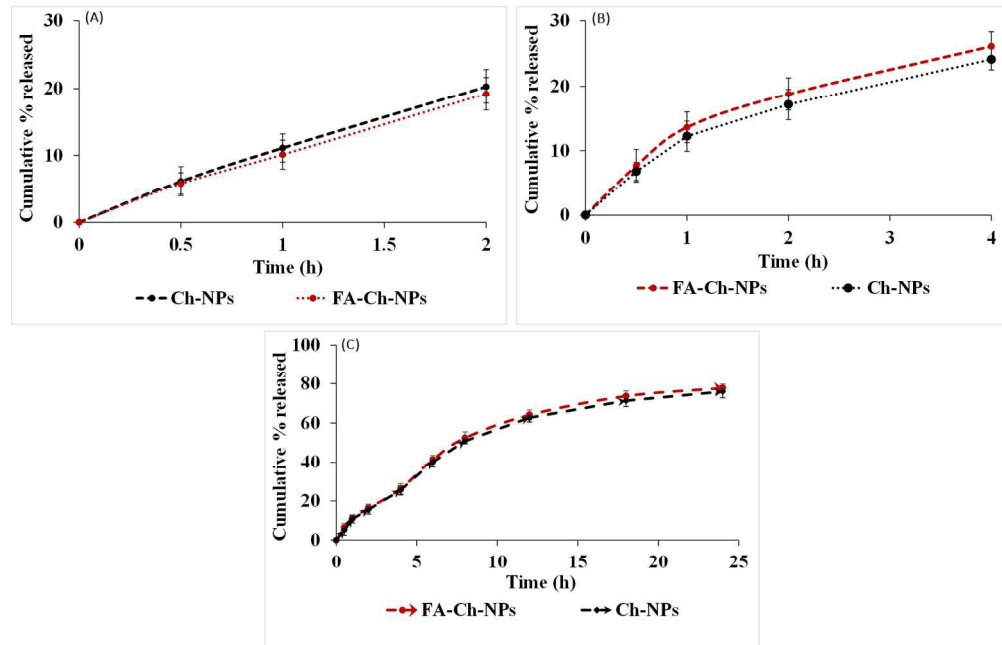
108x35mm (300 x 300 DPI)



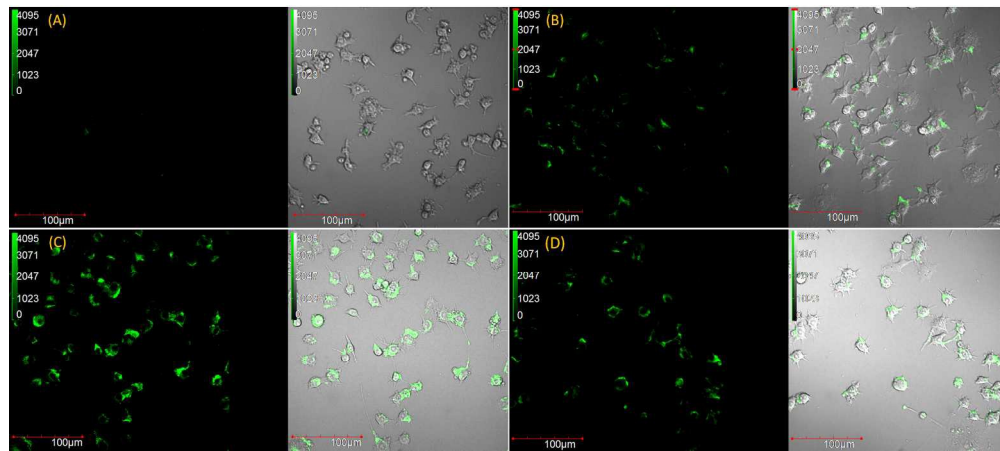
196x49mm (300 x 300 DPI)



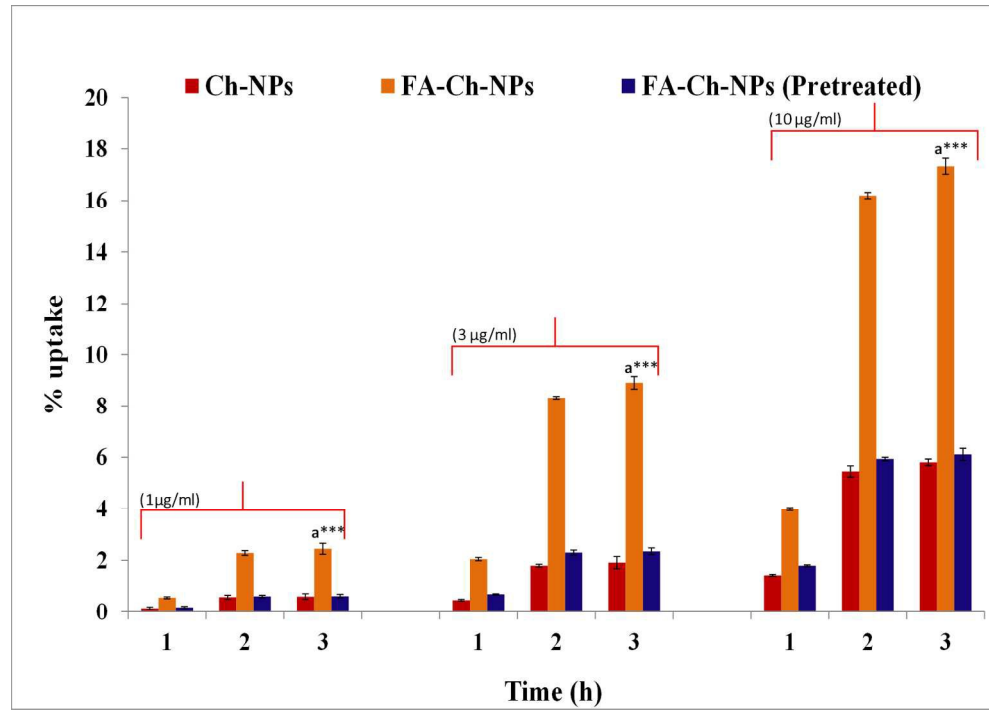
155x90mm (300 x 300 DPI)



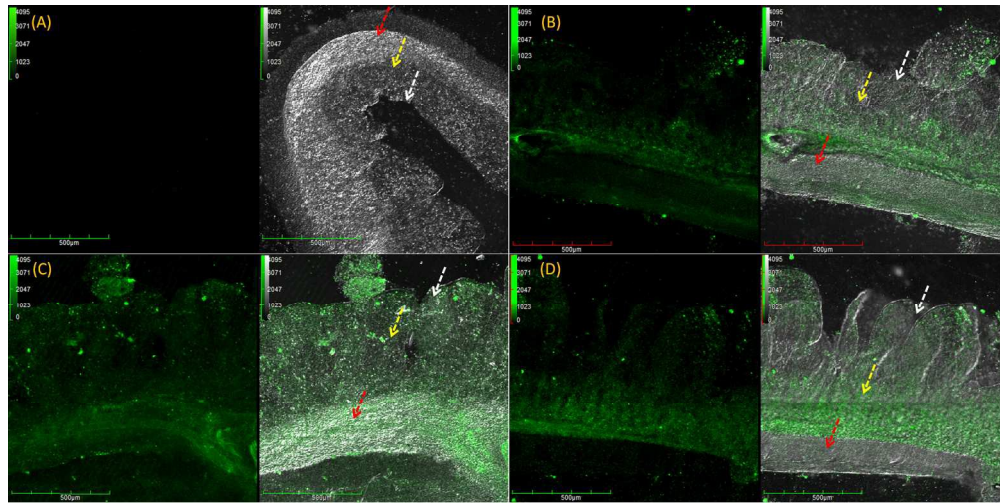
164x106mm (300 x 300 DPI)



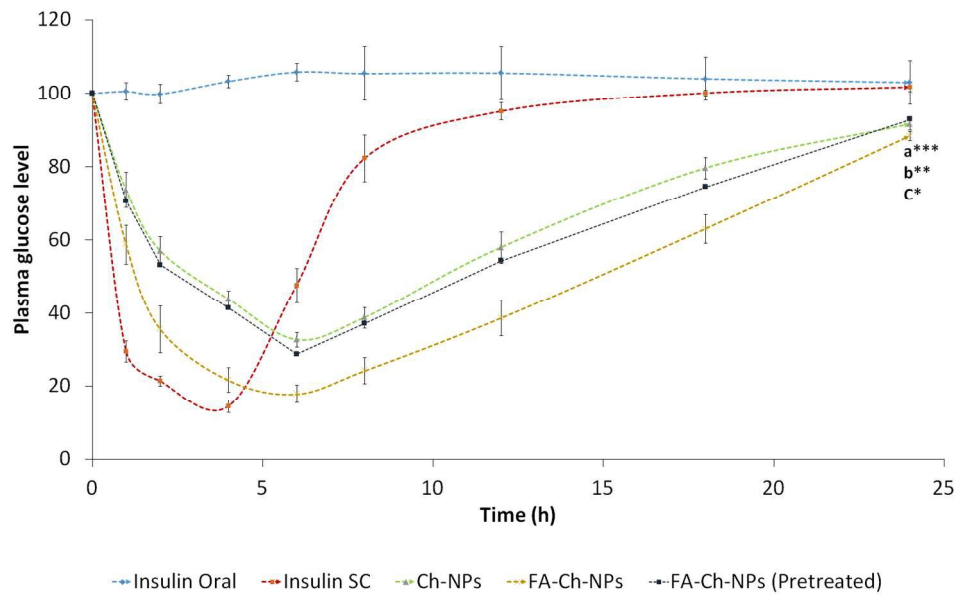
213x94mm (300 x 300 DPI)



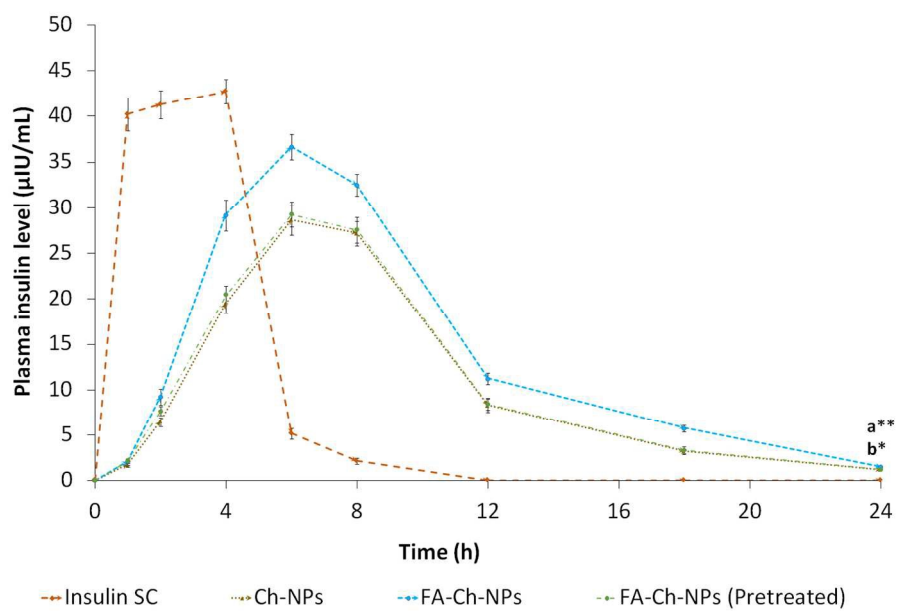
238x168mm (200 x 200 DPI)



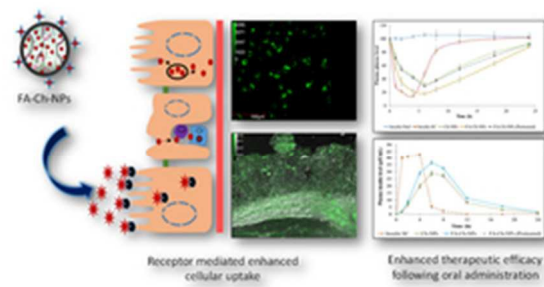
194x96mm (300 x 300 DPI)



151x91mm (300 x 300 DPI)



141x91mm (300 x 300 DPI)



25x13mm (300 x 300 DPI)